AD-A081 103 PENNSYLVANIA STATE UNIV UNIVERSITY PARK APPLIED RESE--ETC F/G 20/4
APPLICATION OF THE STREAMLINE CURVATURE METHOD TO A SOLUTION OF--ETC(U)
AUG 79 M J PIERZGA N00024-79-C-6043
UNCLASSIFIED ARL/PSU/TM-77-244 NL

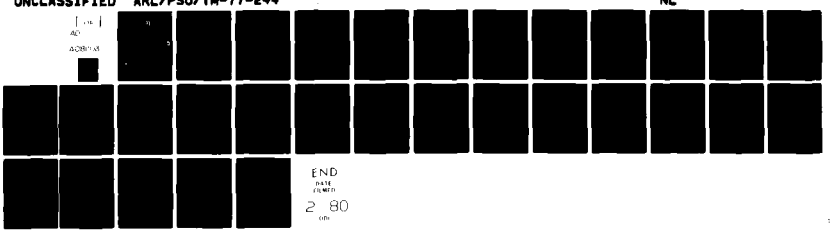

END
DATE FILMED
2 80
DTIC

APPLICATION OF THE STREAMLINE CURVATURE METHOD TO A SOLUTION OF THE DIRECT PROBLEM OF AN OPEN PROPELLER

M. J. Pierzga

Technical Memorandum
File No. TM 77-244
18 August 1977
Contract No. N00024-79-C-6043

Copy No. 14

The Pennsylvania State University
Institute for Science and Engineering
APPLIED RESEARCH LABORATORY
Post Office Box 30
State College, PA 16801

NAVY DEPARTMENT

NAVAL SEA SYSTEMS COMMAND

UNCLASSIFIED

SECURITY CLASSIFICATION OF THIS PAGE *(When Data Entered)*

REPORT DOCUMENTATION PAGE

READ INSTRUCTIONS BEFORE COMPLETING FORM

1. REPORT NUMBER: TM 77-244	2. GOVT ACCESSION NO.
3. RECIPIENT'S CATALOG NUMBER	
4. TITLE *(and Subtitle)*: APPLICATION OF THE STREAMLINE CURVATURE METHOD TO A SOLUTION OF THE DIRECT PROBLEM OF AN OPEN PROPELLER	5. TYPE OF REPORT & PERIOD COVERED: Technical memo
	6. PERFORMING ORG. REPORT NUMBER
7. AUTHOR(s): M. J. Pierzga	8. CONTRACT OR GRANT NUMBER(s): N0024-79-C-6043
9. PERFORMING ORGANIZATION NAME AND ADDRESS: Applied Research Laboratory, P.O. Box 30, State College, PA 16801	10. PROGRAM ELEMENT, PROJECT, TASK AREA & WORK UNIT NUMBERS: 12 372
11. CONTROLLING OFFICE NAME AND ADDRESS: Naval Sea Systems Command, Washington, DC 20362	12. REPORT DATE: 18 Aug 79
	13. NUMBER OF PAGES: 26
14. MONITORING AGENCY NAME & ADDRESS *(if different from Controlling Office)*: 14) ARL/PSU/TM-77-244	15. SECURITY CLASS. *(of this report)*: UNCLASSIFIED
	15a. DECLASSIFICATION/DOWNGRADING SCHEDULE

16. DISTRIBUTION STATEMENT *(of this Report)*

Approved for Public Release. Distribution Unlimited
Per NAVSEA - Feb. 14, 1980.

17. DISTRIBUTION STATEMENT *(of the abstract entered in Block 20, if different from Report)*

18. SUPPLEMENTARY NOTES

19. KEY WORDS *(Continue on reverse side if necessary and identify by block number)*

open, propeller, flow, field, performance, streamline, curvature, method

20. ABSTRACT *(Continue on reverse side if necessary and identify by block number)*

A method is presented of analyzing the flow field and predicting the performance characteristics of an open propeller. The flow field is calculated using the streamline curvature method, an iterative procedure which simultaneously satisfies the principles of conservation of total energy, momentum and continuity. The direct problem solution requires the calculation of the outlet flow angles for the propeller blade sections. These flow angles are a combination of the measured blade outlet angles and the deviation

→ next page

DD FORM 1 JAN 73 1473 EDITION OF 1 NOV 65 IS OBSOLETE

UNCLASSIFIED 391 007

SECURITY CLASSIFICATION OF THIS PAGE *(When Data Entered)*

angles due to real fluid effects. The method of calculating these deviation angles is described in detail. Once the flow field has been established, the propeller performance parameters can then be calculated using simple momentum and energy considerations. Good correlation between predicted data and experimental measurements has been obtained using this direct analysis method.

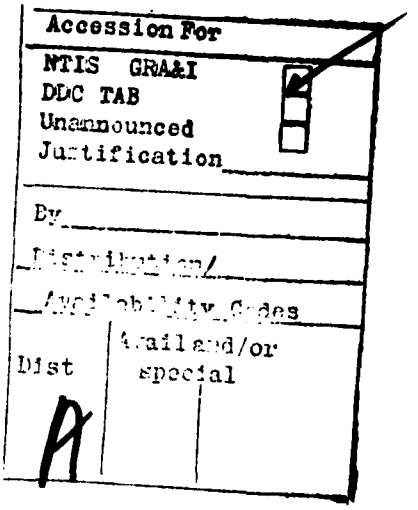

Subject: Application of the Streamline Curvature Method to a Solution of the Direct Problem of an Open Propeller

References: See page 17.

Abstract: A method is presented of analyzing the flow field and predicting the performance characteristics of an open propeller. The flow field is calculated using the streamline curvature method, an iterative procedure which simultaneously satisfies the principles of conservation of total energy, momentum and continuity. The direct problem solution requires the calculation of the outlet flow angles for the propeller blade sections. These flow angles are a combination of the measured blade outlet angles and the deviation angles due to real fluid effects. The method of calculating these deviation angles is described in detail. Once the flow field has been established, the propeller performance parameters can then be calculated using simple momentum and energy considerations. Good correlation between predicted data and experimental measurements has been obtained using this direct analysis method.

Acknowledgement: This work was sponsored by NAVSEA Code 63R31.

List of Symbols

AM	angular momentum
C_P	total pressure coefficient
P	static pressure
R_c	radius of curvature
r	radial position
V_A	axial velocity
V_θ	tangential velocity
V_m	meridional velocity
V_∞	free stream velocity
β_2	outlet flow angle
θ_c	section turning angle
ϕ	flow coefficient
ω	propeller angular velocity

Subscripts and Superscripts

A_p	area of propeller
E	denote propeller exit station
I	denote propeller inlet station
r_i	radius of inner streamline
r_o	radius of bounding streamline
r_p	radius of propeller

I. Introduction

The flow field in an axisymmetric turbomachine can be calculated using either a direct, or an indirect analysis. For the indirect analysis, the propeller designer establishes certain performance objectives such as the required thrust, torque, vehicle speed, or other so-called "design" conditions. With this information, the flow field is calculated and the proper propeller geometry is determined. On the other hand, the direct method deals with the analysis of a propeller with a known geometry. For this case, the flow field and propeller performance data are calculated for design and off-design operating points.

The open propeller is unique in comparison to other types of turbomachines. As the name indicates, this is an "open" machine, i.e., the flow field lacks a well-defined boundary, such as the walls of a turbine or compressor. However, it is possible to consider the flow field for the open propeller as being the region constrained within a potential flow streamtube. The bounding streamsurface of this streamtube is actually located infinitely far from the propeller; however, it is assumed that there is a finite distance at which the flow field is relatively unaffected by the presence of the propeller. This distance is assumed to be at least eight times the propeller radius. The bounding streamline at this distance serves as a flow boundary in this analysis. In this manner, the streamtube becomes analogous to the compressor or turbine duct.

A method which is commonly applied to calculate the flow field in an axisymmetric turbomachine is the streamline curvature method (SLC). This method has been used for some time for the design and analysis of various types of turbomachines. As described by Novak [1], Frost [2], and

Davis [3], this numerical technique has been successfully used for the indirect analyses of compressors and turbines. Also, McBride [4] has applied this streamline curvature method to the indirect problem of an open hydrodynamic propeller. However, very little work has been done using the streamline curvature method for the direct open propeller problem.

It is the objective of this paper to discuss a method which can be used to solve the direct open propeller problem. The streamline curvature technique used to establish the streamlines in the propeller flow field is discussed in detail.

II. Streamline Curvature Method

Basic Equations

The major equations used in the streamline curvature method of analysis are derived from the principles of conservation of mass, momentum, and total energy. The equations which are used are generalized for an axisymmetric flow field and allow for curvature of the streamlines. The working fluid in this analysis is assumed to be incompressible, inviscid and steady. Thus, the equations are derived with these assumptions in mind.

One of the fundamental equations used in the analysis is obtained from the principle of conservation of mass within a streamtube. The continuity equation states that for a steady flow,

$$\int_{c.s.} \rho V \, dA = 0 \quad . \tag{1}$$

This integral is evaluated over a control surface where V is the velocity

component normal to the element of surface area (dA). By using a streamtube as the control volume, there is no transport of mass normal to the streamsurface. Thus, the continuity equation for an incompressible flow within a streamtube can be simplified to

$$2\pi \int_{in}^{out} V_A \, r \, dr = 0 \quad , \tag{2}$$

where the integral is evaluated from some inlet station to an exit station along the streamtube. Because the areas represented by this form of the continuity equation are located in radial planes, the component of velocity is necessarily in the axial direction (V_A).

For this axisymmetric analysis, it is necessary to use only the components of total velocity in two directions. The component of velocity which is tangent to the streamline and is projected onto the meridional plane is called the meridional velocity (V_m). This component of total velocity is related to the axial component by the cosine of the streamline angle (α). The second component of total velocity is known as the tangential velocity (V_θ), and it is located in the circumferential direction, which is perpendicular to the meridional plane. These velocity components as well as the computational coordinate system are illustrated in Figures 1a and 1b.

Meridional curvature of the streamlines in the flow tends to disrupt the equilibrium along a streamline. To satisfy the principle of conservation of momentum, a radial static pressure gradient develops. There are really three contributing factors in the development of this pressure gradient. The first term is indeed due to the moving particle being subjected to the streamline curvature in the meridional plane.

The magnitude of this term depends greatly on the radius of curvature of the streamline at a specific location (R_c). The second term is directly related to the centrifugal force which the rotating fluid experiences upon passing through the propeller blades. The final term is proportional to the convective acceleration of the fluid particle as the flow area either converges or diverges. The combination of these three terms is known as the radial equilibrium equation and is expressed as

$$\frac{dP}{\rho} = \left\{ \frac{V_m^2}{R_c} dn + \frac{V_\theta^2}{r} dr - V_m \frac{\partial V_m}{\partial S} ds \right\} \quad . \tag{3}$$

It can be seen that for an axial flow turbomachine with no streamline curvature and no variation in flow area, Equation (3) reduces to the simplified version of the radial equilibrium equation.

Because total energy must be conserved along a streamline, the total energy between two points on a streamline, upstream or downstream of the propeller but not across the propeller, can be written in terms of the total pressures

$$P_1 + 1/2\rho\, V_1^2 = P_\eta + 1/2\rho\, V_\eta^2 \quad , \tag{4}$$

where the subscript (1) indicates a station of known total pressure and the subscript (η) indicates an arbitrary station. This equation is seen to be Bernoulli's equation along a streamline for an inviscid flow. A simplification to this equation is possible by expressing the total velocity (V_η) in its components and by realizing that

$$P_\eta = P_{\eta_i} + \int_{\eta_i}^{\eta_o} dP \quad , \tag{5}$$

where P_{η_i} is the absolute static pressure on the innermost streamline for a given station in the flow field. The integral of the radial equilibrium equation yields the static pressure difference between the inner streamline (η_i) and an arbitrary outer streamline (η_o). Using Equation (5) and rearranging Equation (4), an expression for the meridional velocity is obtained:

$$1/2\rho\ V_m^2 = P_1 + 1/2\rho\ V_1^2 - P_{\eta_i} - \int_{\eta_i}^{\eta_o} dP - 1/2\rho\ V_\theta^2 \quad . \tag{6}$$

Normally, this form of the energy equation cannot be solved since there are two unknowns, namely, P_{η_i} and V_m. However, by using continuity and eliminating the meridional velocity term, the static pressure on the inner streamline (P_{η_i}) can be computed. Once this value is known, a new meridional velocity profile which satisfies the energy equation can be calculated for each station in the flow field using Equation (6).

The three equations, continuity, radial equilibrium, and energy, are the basis for the flow field solution obtained by the streamline curvature method.

Boundary Conditions

The streamline curvature method uses an iterative procedure to obtain a flow field solution which simultaneously satisfies the three basic equations. The iteration procedure can be long and laborious. For this reason, an indirect streamline curvature computer program developed by McBride [5] has been modified to solve the direct problem of the open propeller. A flow diagram of the major computational steps is shown in Figure 2.

As the first two blocks in the flow diagram indicate, there are two initial boundary conditions which must be known before the computational process can proceed. The first boundary condition is that the flow energy must be known at some reference station far upstream of the propeller. This flow energy is usually specified in terms of the components of total velocity. Knowing the meridional and tangential velocity distributions along some reference station line, the total energy along any streamline can be calculated and must remain constant until it is changed by the propeller. This change in energy through the propeller is the other boundary condition. In the direct analysis, the energy along a streamline coming out of the propeller is related to the angle at which the flow exits from the propeller blade at each streamline position. These exit flow angles must be known before any estimation of the energy change through the propeller is made.

The determination of these exit flow angles is the heart of this computational method. The ideal outlet flow angle is simply the fixed angle between the tangent to the camberline at the trailing edge of a blade section and the exit axial velocity vector. This angle is shown in Figure 3. This ideal outlet flow angle however, is not the angle at which a real fluid exits from the blade row.

The calculation of the deviation term which allows for real flow effects is a necessary boundary condition for the direct problem. A method for estimating a deviation angle will be discussed in a later section. For the present, it is assumed that the measured outlet flow angles and the correct deviation terms have been computed and are used as the second boundary condition for the analysis.

Computational Procedure

As the flow diagram in Figure 2 indicates, the initial velocity distributions at the reference station must be transferred to the downstream flow stations so that an initial flow field can be established. This transfer is carried out in three steps. First, the meridional velocity profile is transferred throughout the flow field by means of the continuity equation. Second, the reference tangential velocity distribution is transferred through the flow field to the propeller inlet station by means of conservation of angular momentum. Since the propeller changes the angular momentum along a streamline, the tangential velocity profile at the propeller exit station must be obtained to allow for further calculations. This is where the second boundary condition enters the analysis. From Figure 3, it can be seen that the outlet flow angle (β_2) is related to the tangential velocity by the equation

$$V_\theta = \omega r - V_{A_2} \tan \beta_2 \quad , \tag{7}$$

where ωr is the angular velocity of the propeller and V_{A_2} is the axial velocity at the propeller exit station. Knowing the outlet flow angles enables the values of tangential velocity to be computed at the propeller exit station. Once the angular momentum at this station is calculated, the principle of constant angular momentum allows for the third step to be carried out; the transfer of tangential velocity downstream of the propeller.

After the initial meridional profile has been transferred downstream, the initial streamline locations can be determined. Locating the streamlines is accomplished by using a streamline spacing function.

This function assigns a specific percentage of the total mass flow to each streamline, thereby establishing a unique radial position for each streamline along every station in the flow field. These points are then fit with a line which represents the individual streamline.

At this point, the flow field has been established based on the two boundary conditions and continuity. The solution, however, must also satisfy radial equilibrium and total energy requirements. The pressure gradient given by the radial equilibrium equation (Equation (3)) is computed at every station from the inner streamline to the bounding streamsurface. To obtain the static pressure on the inner streamline, it is necessary to combine the energy equation (Equation (6)) and continuity equation (Equation (2)). The stations upstream of the propeller are calculated based on the known total pressures at the reference station. The static pressure at stations downstream of the propeller require the calculation of total pressures (static plus dynamic) along a streamline at the propeller exit station. This calculation is obtained from an angular momentum change. Angular momentum is defined along a streamline as the tangential component of velocity multiplied by its radial distance. Knowing the angular momentum before and after the propeller, the total pressure in coefficient form at the exit station is given by,

$$C_{P_E} = C_{P_I} + \frac{8\pi^2}{\phi V_\infty r_p} (AM_E - AM_I) \qquad (8)$$

where C_{P_E} is the total pressure coefficient at the propeller exit station. This equation yields the increase in total pressure across the propeller along a streamline.

Having computed the total pressure at the exit station, it is now possible to calculate a new meridional velocity profile for every downstream station which satisfies total energy conservation (Equation (6)). This new velocity profile is then integrated for a new mass flow distribution. Using the streamline spacing function and this new distribution of mass flow, new streamline locations are calculated and the entire set of streamlines is repositioned.

The convergence criterion for this iteration procedure is related to the amount of shifting that any particular streamline experiences. If the shift of every streamline is within prescribed limits, the solution is said to be converged and the iteration cycle is complete. If the shift of any streamline is not within the specified tolerance, the procedure continues its iteration cycle as shown by the flow diagram in Figure 2. Upon convergence, the flow field simultaneously satisfies continuity, conservation of momentum, and conservation of total energy.

Once the flow field has been calculated, the performance parameters, such as thrust and torque, can be computed based on energy and momentum considerations. The torque coefficient is defined as

$$C_Q = \int_{r_i}^{r_o} \frac{2\pi\ AM_E\ V_{m_E}\ r\ dn}{1/2\ \ V_\infty^2\ A_p\ r_p} - \int_{r_i}^{r_o} \frac{2\pi\ AM_I\ V_{m_I}\ r\ dn}{1/2\ \ V_\infty^2\ A_p\ r_p} \quad . \tag{9}$$

This torque coefficient gives an indication as to the size requirements for the powerplant to be used in conjunction with a specific propeller.

A measure of the forward force produced by the propeller is in the form of a thrust coefficient. The thrust coefficient can be obtained by means of actuator disc theory. In this analysis, the rotating blade row is modeled by a solid actuator disc and the momentum equation yields

the resultant force in coefficient form as

$$C_T = \int_{r_i}^{r_p} 2\pi \left\{ \left[P_{\eta_i} + \int_{\eta_i}^{\eta_o} dP \right]_E - \left[P_{\eta_i} + \int_{\eta_i}^{\eta_o} dP \right]_I \right\} \frac{r\, dr}{1/2\rho\, V_\infty^2\, A_p} \quad . \qquad (10)$$

III. Outlet Flow Angles

Calculation of Deviation Angles

The propeller outlet flow angle is defined as the angle between the tangent to the blade section camberline at the trailing edge and the exit axial velocity vector. This measurable angle is the angle which the flow would follow if there were no viscous effects and the flow behaved as a perfect fluid. Unfortunately, a real flow will not follow this ideal angle; therefore, corrections in the form of deviation angles must be computed. The accurate determination of these outlet deviation angles allows this analysis to model a real flow with viscous as well as secondary flow effects.

The procedure for calculating the final deviation angles involves running the streamline curvature (SLC) program a total of three times. The entire procedure is outlined in the flow diagram in Figure 4. Each "run" of the SLC program adds subsequent terms to the total deviation. For the initial run of the program, the section outlet angles are measured and added to a deviation term (δ_H) developed by Howell[6]. This deviation angle is defined for each blade section as

$$\delta_H = \frac{0.23\ (\theta_c)(s/c)^{1/2}(2a/c)^2}{1.0 - (0.1/50)(\theta_c)(s/c)^{1/2}} \qquad (11)$$

where, θ_c is the section turning angle, s/c is the space-to-chord ratio, and a/c is the distance from the section leading edge to the point of maximum camber divided by the section chord length.

Once a converged solution is obtained for the flow field using Howell's deviation, the axial velocity distributions can be used to calculate an improved deviation term. The effect of flow acceleration, blade camber and blade thickness can now be calculated separately. The deviation term due to axial accelerations through the propeller is given by Lakshminarayana [7] as,

$$\Delta\delta' = \frac{AVR-1.0}{AVR}\left\{\right.$$

$$\left\{\frac{\pi K(c/s)(G/c+\alpha/4)\cos[(\beta_1+\beta_2)/2][(AVR+1)^2-4]}{8+\pi K(c/s)(\alpha/4+G/c)\cos[(\beta_1+\beta_2)/2][(AVR+1)\tan\beta_2+2\tan\beta_1]}\right.$$

$$\left.-\frac{\frac{2\pi K(c/s)\tan\beta_1}{AVR\cos[(\beta_1+\beta_2)/2]\sec^2\beta_1}}{8+\pi K(c/s)(\alpha/4+G/c)\cos[(\beta_1+\beta_2)/2][(AVR+1)\tan\beta_2+2\tan\beta_1]}\right\}$$

$$\left.+\tan\beta_2\right\}\cos^2\beta_2 \qquad (12)$$

where AVR is the axial velocity ratio (V_{A_2}/V_{A_1}), K is the cascade influence coefficient[8], G/c is the distance from the chordline to the maximum camber point of the section divided by the chord length, β_1 and β_2 are the inlet and outlet flow angles, respectively, and α is defined as the difference between the inlet flow angle (β_1) and the section stagger angle (λ).

Howell's deviation formula considers only thin blade sections; therefore, a separate term due to thickness effects must also be calculated. This deviation term is given by empirical data which has been collected by the National Aeronautics and Space Administration[9]. This term is calculated from the equation,

$$\Delta\delta^* = (K_\delta)_{sh} \cdot (K_\delta)_t \cdot (\delta_o^\circ)_{10} \quad . \tag{13}$$

The terms on the right-hand side of Equation (13) are determined from graphs of experimental data based on section solidity and inlet flow angles. Also given in NASA's development of deviation terms is a better approximation of the effect of camber based on empirical data. This term replaces Howell's deviation term. From graphs of section solidity and inlet flow angles, a value for the slope, m, is obtained and used to calculate this deviation term

$$\delta_o = m \cdot \theta_c \quad . \tag{14}$$

Knowing these terms of the deviation angle due to axial acceleration effects, blade thickness and the improved camber deviation, one calculates a new outlet flow angle profile from

$$\beta_2^* = \beta_2 - \Delta\delta' + \Delta\delta^* + \delta_o \quad . \tag{15}$$

This new outlet flow angle profile is then used in the SLC program for the second run of this three part calculation.

The results of this converged solution are then used to solve secondary vorticity equations and to determine a deviation term ($\Delta\delta_s$) which is due to secondary flow effects as described by Billet[10]. The final outlet flow angle profile is obtained by adding this secondary flow term to the deviation terms thus far calculated to obtain

$$\beta_2^{**} = \beta_2 - \Delta\delta' + \Delta\delta^* + \delta_o + \Delta\delta_s \quad . \tag{16}$$

This final outlet flow angle distribution is then used as the second boundary condition in the last run of the SLC program. Obtaining the deviation angle by this complex procedure enables the modeling of a real fluid flowing through a real propeller.

Comparison of Results

To verify the accuracy of this direct analysis method, two test cases were calculated. In the first case, the flow field was calculated for an open propeller operating at its design conditions. This implies a specific propeller flow coefficient given as,

$$\phi = \frac{V_\infty}{\omega r_p} \tag{17}$$

where the design thrust and torque are achieved. For the second test case, the same propeller was operating at a 10% reduction of flow coefficient.

These two cases were chosen because experimental data were available from other investigations (References 11 and 12). The inlet and exit velocity profiles had been measured in tests conducted in the 48-inch water tunnel and the 48-inch wind tunnel at the Garfield Thomas Water Tunnel at The Pennsylvania State University.

The comparison between experimental data and analytical predictions are shown in Figures 5 through 8. For each test case two figures are shown. The first figure in each case shows the axial velocity profile at the inlet station to the propeller. These two figures show somewhat similar trends even though one is the design case, Figure 5, and one is the 10% off-design case, Figure 7. In these figures the predicted data agree very well with values obtained experimentally. Some deviation is noticed in the region of the propeller hub. This overprediction close to the hub is due to the inability of the SLC program to handle very small velocities in this region. Low velocities produce program instabilities and have to be handled very carefully. This stability problem is of importance only on the first two or three streamlines and, as the figures verify, has no effect on the outer positions of the flow.

The second figure in each of the test cases, Figures 6 and 8, shows the velocity components as a function of radial distance from the propeller hub at the propeller exit station. The design test case, Figure 6, shows good correlation between the predicted and the experimental axial velocity data. The bulge in the axial velocity profile is due to the contraction of the streamlines as they pass through the propeller. This contraction is a result of the work done by the propeller in the region of high blade loading.

The remaining plot in Figure 6 is a comparison between the predicted and the experimental tangential velocity distribution at the propeller exit station. In this case the two curves are not as close as the axial velocity curves especially near the hub. The deviation near the hub is attributed to the overprediction, Figure 5, of the inlet velocity profile in this same region. It should also be pointed out that in the region

of the propeller tip the flow is highly three-dimensional and experimental data may be expected to deviate slightly from data predicted by the analytical technique.

The 10% off-design case, Figure 8, shows similar trends as discussed for the design case even though the absolute magnitudes of the data are different. Again, the correlation between experimental and analytical data is very good but with small deviations near the hub of the tangential velocity curve.

IV. SUMMARY

A numerical solution to the direct problem has been developed for calculating the flow field of an open propeller using the streamline curvature method. Results were obtained which closely model the flow by implementing the streamline curvature technique to solve the equations of motion through the turbomachine. By making adjustments to the outlet flow angles to allow for viscous and secondary flow effects, good correlation between experimental measurements and theoretical predictions have resulted. The degree of accuracy which has been experienced thus far indicates that this method can be a valuable tool in the performance predications of a propeller operating at other than design conditions. Consequently, this method has the capacity to give the engineer a clear picture of how a particular propeller will act at off-design conditions without going through the time and expense of experimental testing.

REFERENCES

[1]Novak, R. A., "Streamline Curvature Computing Procedures," Journal of Engineering for Power, Trans. ASME, Series A, Vol. 89, No. 4, October 1967, pp. 478-490.

[2]Frost, D. H., "A Streamline Curvature Through-Flow Computer Program for Analyzing the Flow Through Axial Flow Turbomachines," A.R.C. R&M No. 3687, August 1970.

[3]Davis, W. R., "A Computer Program for the Analysis and Design of Turbomachinery -- Revision," Carleton University, Report No. ME/A 71-5.

[4]McBride, M. W., "Refinement of the Mean Streamline Method of Blade Section Design," ASME Paper No. 76-WA/FE11, New York, NY.

[5]McBride, M. W., Conversations with Mr. McBride, Applied Research Laboratory, The Pennsylvania State University (1976-1977).

[6]Horlock, J. H., "Two Dimensional Cascades: Experimental Work," Axial Flow Compressors, Robert E. Krieger, New York, 1973, pp. 55-60.

[7]Lakshminarayana, B., A Discussion of Wilson, Mani, and Acosta's, "A Note on the Influence of Axial Velocity Ratios on Cascade Performance," NASA SP-304, Part I, 1974, pp. 127-133.

[8]Scholz, N., Aerodynamik der Schaufelgitter, Band I, Verlag G. Braun, p. 165.

[9]Lieblein, S., "Experimental Flow in Two-Dimensional Cascades," NASA SP-36, Part I, 1974, pp. 127-133.

[10]Billet, M. L., "Secondary-Flow-Related Vortex Cavitation," Applied Research Laboratory, Technical Memorandum File No. TM 78-189, July 5, 1978.

[11]Billet, M. L., "Rotor Incoming Velocity Profiles Measurements," Applied Research Laboratory, Technical Memorandum File No. TM 76-254, October 11, 1976.

[12]Billet, M. L., "Flow Measurements Behind a Rotor Operating in a Boundary Layer, Applied Research Laboratory, Technical Memorandum File No. TM 76-260, October 12, 1976.

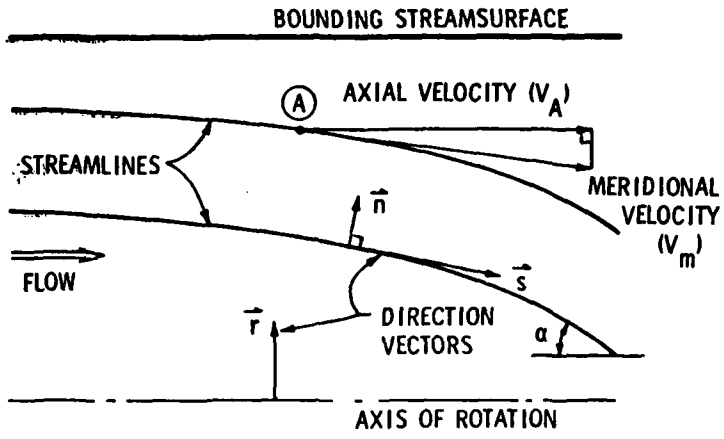

Figure 1a - Velocity Components and Coordinate System as Seen in a Side View of Flow Field (Meridional Plane)

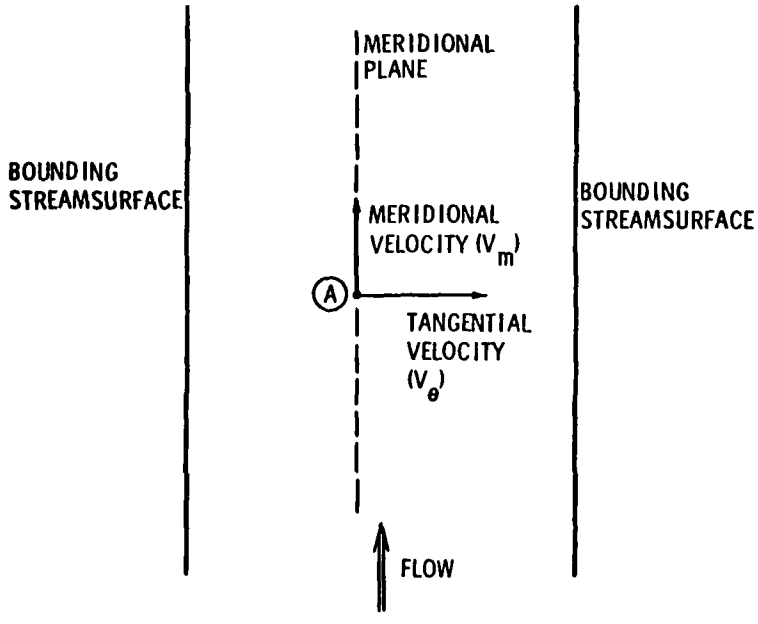

Figure 1b - Velocity Components as Seen in a Top View of Flow Field

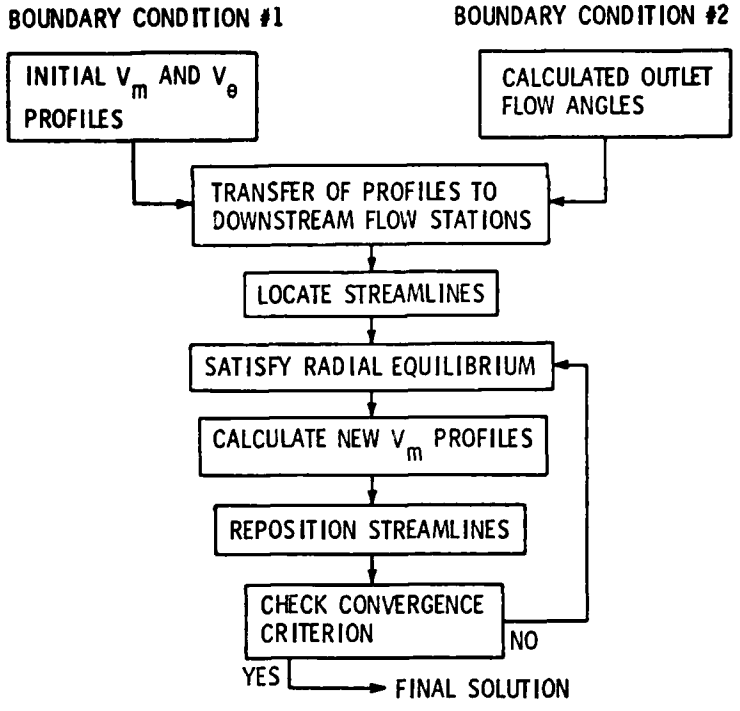

Figure 2 - A Flow Diagram of SLC Computational Procedure

18 August 1977
MJP:jep

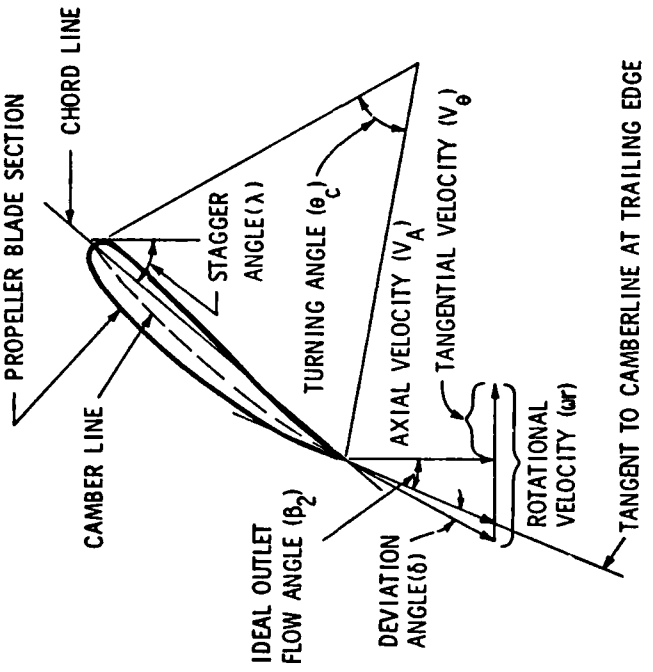

Figure 3 - Propeller Section Geometry

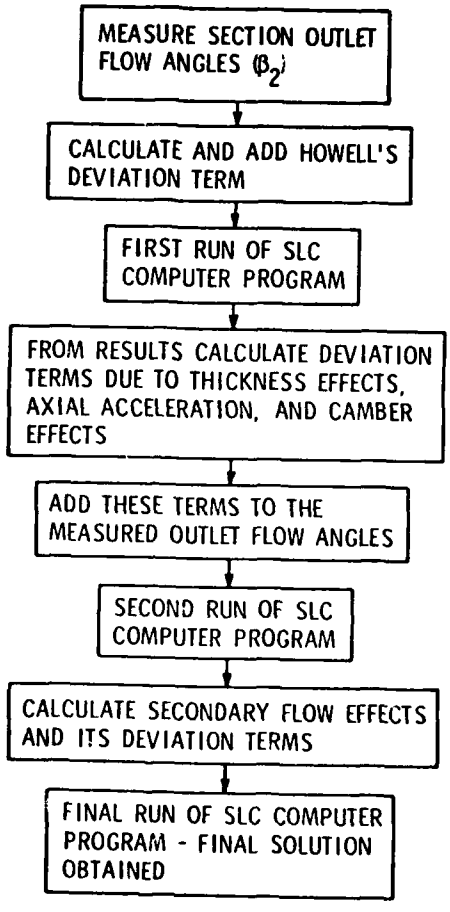

Figure 4 - A Flow Diagram of the Procedure Used to Calculate the Deviation Angles

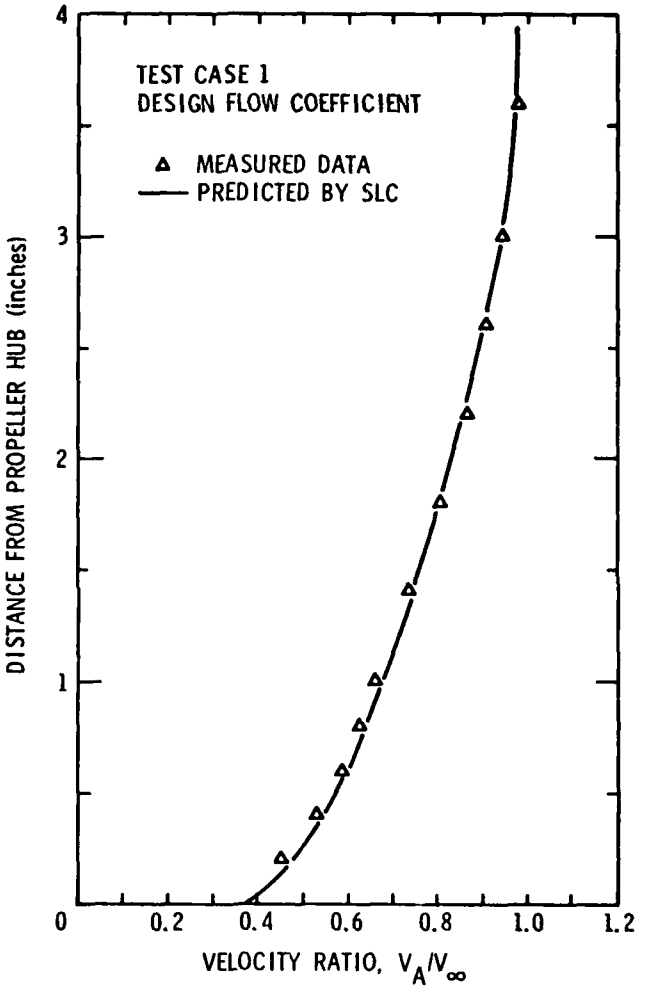

Figure 5 - Comparison of Measured and Predicted Velocity Profile at Propeller Inlet Station for Design Conditions

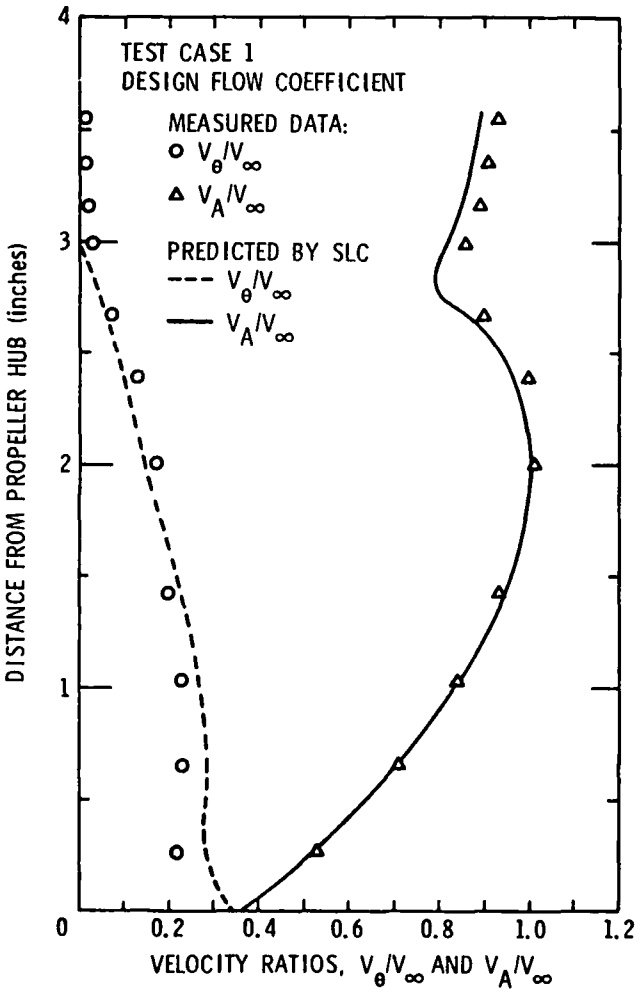

Figure 6 - Comparison of Measured and Predicted Velocity Profiles at Propeller Exit Station for Design Conditions

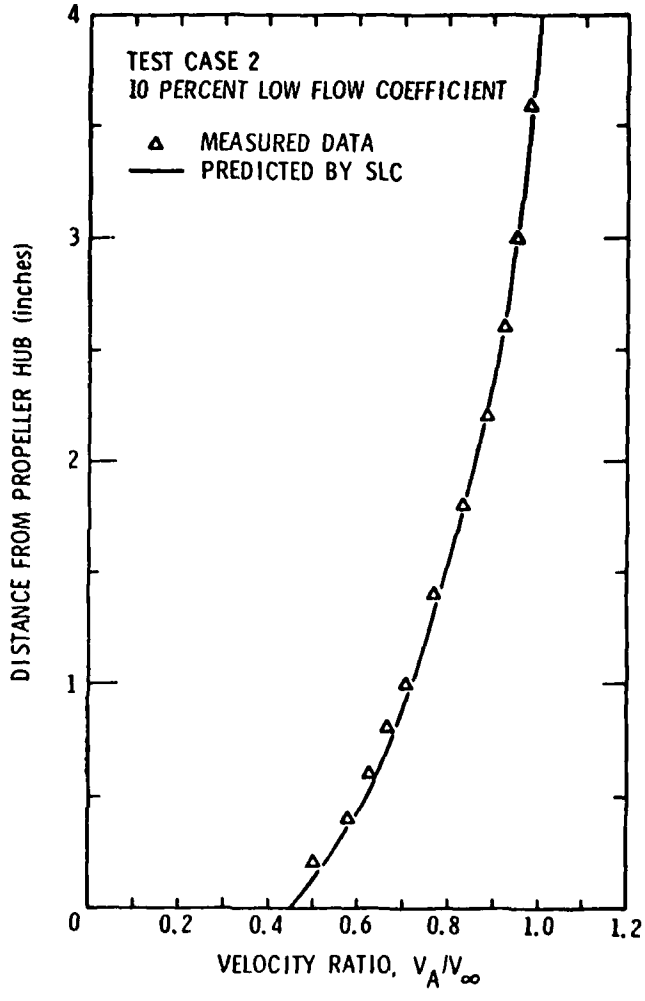

Figure 7 - Comparison of Measured and Predicted Velocity Profile at Propeller Inlet Station for 10% Off-Design Conditions

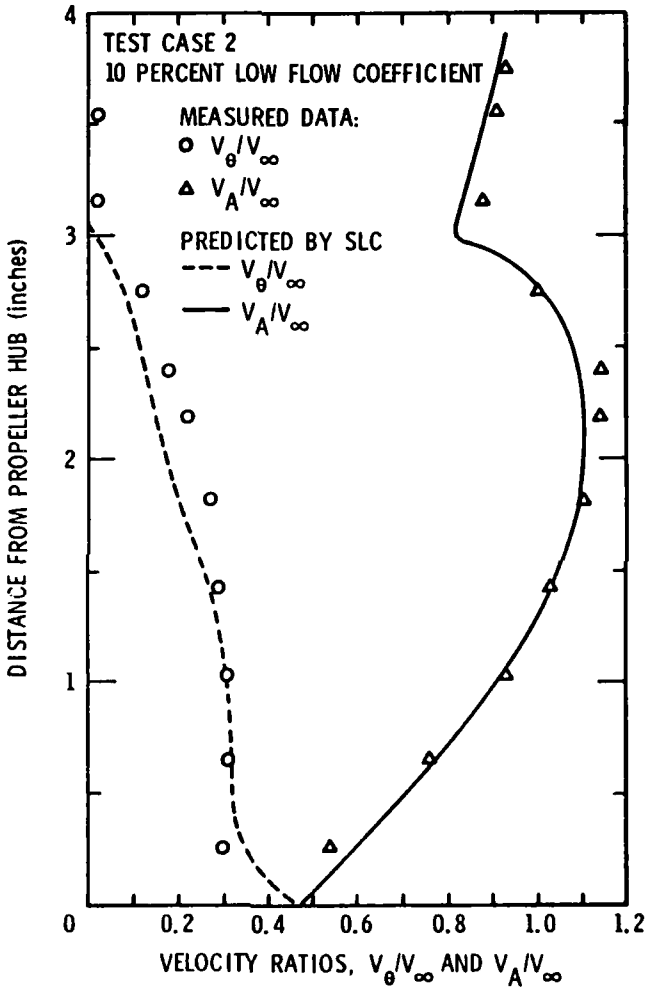

Figure 8 - Comparison of Measured and Predicted Velocity Profiles at Propeller Exit Station for 10% Off-Design Conditions

DISTRIBUTION LIST FOR UNCLASSIFIED TM 77-244 by M. J. Pierzga, dated 18 August 1977

Commander
Naval Sea Systems Command
Department of the Navy
Washington, DC 20362
Attn: T. E. Peirce
Code NSEA-63R3
(Copy No. 1)

Naval Sea Systems Command
Attn: A. R. Paladino
Code NSEA-05H1
(Copy No. 2)

Commanding Officer
Naval Underwater Systems Center
Newport, RI 02840
Attn: Library
Code 54
(Copy No. 3)

Commanding Officer
Naval Ocean Systems Center
San Diego, CA 92152
Attn: D. Nelson
Code 6342
(Copy No. 4)

Naval Ocean Systems Center
Attn: M. M. Rieschman
Code 2542
(Copy No. 5)

Commander
David W. Taylor Naval Ship R&D Center
Department of the Navy
Bethesda, MD 20084
Attn: T. E. Brockett
Code 1544
(Copy No. 6)

David W. Taylor Naval Ship R&D Center
Attn: R. A. Cumming
Code 1544
(Copy No. 7)

David W. Taylor Naval Ship R&D Center
Attn: J. H. McCarthy
Code 1552
(Copy No. 8)

David W. Taylor Naval Ship R&D Center
Attn: W. B. Morgan
Code 154
(Copy No. 9)

David W. Taylor Naval Ship R&D Center
Attn: F. Peterson
Code 1500
(Copy No. 10)

David W. Taylor Naval Ship R&D Center
Attn: R. Rothblum
Code 1556
(Copy No. 11)

David W. Taylor Naval Ship R&D Center
Attn: M. M. Sevik
Code 19
(Copy No. 12)

Office-In-Charge
David W. Taylor Naval Ship R&D Center
Department of the Navy
Annapolis Laboratory
Annapolis, MD 21402
Attn: J. G. Stricker
Code 2721
(Copy No. 13)

Defense Documentation Center
5010 Duke Street
Cameron Station
Alexandria, VA 22314
(Copies No. 14 - 25)

NASA Lewis Research Center
21000 Brookpark Road
Cleveland, Ohio 44135
Attn: W. M. McNally, MS 5-9
(Copy No. 26)

NASA Lewis Research Center
Attn: N. C. Sanger, MS 5-9
(Copy No. 27)

NASA Lewis Research Center
Attn: M. J. Pierzga, MS 5-9
(Copy No. 28)

Dr. Bruce D. Cox
Stevens Institute of Technology
Davidson Laboratory
Castle Point Station
Hoboken, NJ 07030
(Copy No. 29)

Allis-Chalmers Corp.
Hydro-Turbine Division
Box 712
York, PA 17405
Attn: R. K. Fisher
(Copy No. 30)

DISTRIBUTION LIST FOR UNCLASSIFIED TM 77-244 by M. J. Pierzga, dated 18 August 1977

Dr. W. van Gent
Netherlands Ship Model Basin
Haagsteeg 2
P.O. Box 28
67 AA Wageningen
The Netherlands
(Copy No. 31)

Dr. Peter van Oossanen
Netherlands Ship Model Basin
Haagsteeg 2
P.O. Box 28
67 AA Wageningen
The Netherlands
(Copy No. 32)

Dr. rer. nat. Horst Merbt
Forschungsbeauftragter fur Hydroakustik
8012 Ottobrunn B. Munchen
Waldparkstr. 41
Munich
Germany
(Copy No. 33)

Mr. H. J. Baiter
Fraunhofer-Institut fur Hydroakustik
Postfach 260
8013 Ottobrunn
Fed. Rep. of Germany
(Copy No. 34)

Dr. Allen Moore
Admiralty Research Laboratory
Teddington, Middlesex
England
(Copy No. 35)

Dr. John H. Horlock
Vice Chancellor
University of Salford
Salford, M5 4WT
England
(Copy No. 36)

Hydronautics, Inc.
Pindell School Road
Laurel, MD 20810
(Copy No. 37)

The Pennsylvania State University
Applied Research Laboratory
Post Office Box 30
State College, PA 16801
Attn: W. S. Gearhart
(Copy No. 38)

Applied Research Laboratory
Attn: R. E. Henderson
(Copy No. 39)

Applied Research Laboratory
Attn: M. W. McBride
(Copy No. 40)

Applied Research Laboratory
Attn: M. L. Billet
(Copy No. 41)

Applied Research Laboratory
Attn: GTWT Library
(Copy No. 42)